International Journal of Chronic Obstructive Pulmonary Disease Dovepress
open access to scientific and medical research

Open Access Full Text Article

ORIGINAL RESEARCH

MiR-361-5p/*abca1* and MiR-196-5p/*arhgef12* Axis Involved in γ-Sitosterol Inducing Dual Anti-Proliferative Effects on Bronchial Epithelial Cells of Chronic Obstructive Pulmonary Disease

Hui-fen Shen[1,*]
Ying Liu[1,*]
Ping-ping Qu[1]
Yu Tang[1]
Bing-bing Li[2]
Guo-liang Cheng[2]

[1]Yantai Affiliated Hospital of Binzhou Medical University, Yantai, 264000, People's Republic of China; [2]State Key Laboratory of Generic Manufacture Technology of Chinese Traditional Medicine, Lunan Pharmaceutical Group Co. Ltd., Linyi, 276006, People's Republic of China

*These authors contributed equally to this work

Purpose: Chronic obstructive pulmonary disease (COPD), a progressive and irreversible respiratory disease, becomes the third leading cause of death and results in enormous economic burden on healthcare costs and productivity loss worldwide by 2020. Thus, it is urgent to develop effective anti-COPD drugs.

Materials and Methods: In the present study, two published GEO profiles were used to re-analyze and ascertain the relationships between circulating miRNAs and bronchial epithelial cells (BECs) mRNAs in COPD. The microRNA levels of miR-361-5p and miR-196-5p in plasma of COPD patients and healthy volunteers were detected by qRT-PCR. Next, the effects of γ-sitosterol (GS) on the expression of miR-361-5p and miR-196-5p and cell proliferation were investigated in BEC and H292 cell lines. Finally, whether specific miRNA-mRNA pathways involved in the effect of GS on BECs was assayed using Western Blot, real-time PCR and immunofluorescence.

Results: miR-196-5p and miR-361-5p were, respectively, up- and down-regulated in COPD patients compared with healthy controls. Luciferase assays demonstrated that miR-361-5p and miR-196-5p were, respectively, targeting *abca1* and *arhgef12* 3′UTR in BEAS-2B cells. GS significantly suppressed miR-196-5p and promoted miR-361-5p levels in BEAS-2B cells and inhibited BECs proliferation in vitro. GS promoted miR-361-5p expression, which inhibited BCAT1 mRNA and protein levels and weaken mTOR-pS6K pathway, resulted in anti-proliferation in BEAS-2B cells. In addition, RhoA was activated by ARHGEF12 due to the inhibitory effect of miR-196-5p on *arhgef12*-3′UTR which was partially abolished by GS suppressing miR-196-5p expression. Activated RhoA further activated ROCK1-PTEN pathway and finally inhibited mTOR pathway, resulting in induced BECs proliferation. The anti-proliferation effect of GS was not observed in H292 cells.

Conclusion: These findings indicate that miR-361-5p/*abca1* and miR-196-5p/*arhgef12* axis mediated GS inducing dual anti-proliferation effects on BECs.

Keywords: chronic obstructive pulmonary disease, γ-sitosterol, miR-361-5p, *abca1*, miR-196-5p, *arhgef12*

Correspondence: Guo-liang Cheng; Bing-bing Li
State Key Laboratory of Generic Manufacture Technology of Chinese Traditional Medicine, Lunan Pharmaceutical Group Co. Ltd., Hongqi Road No. 209, Linyi, 276006, Shandong, People's Republic of China
Email september1984@aliyun.com; libingt@126.com

Introduction

As the first line of defense against airway inflammation, the disequilibrium between injury and repair of bronchial epithelial cells (BECs) is common in patients suffering from various lung diseases[1] including chronic obstructive pulmonary disease (COPD),[2] and is associated with increased risk of lung cancer.[3]

Received: 8 July 2021
Accepted: 27 September 2021
Published: 5 October 2021

COPD is one of the primary causes of morbidity and mortality worldwide which is usually characterized by progressive, irreversible airway obstruction, resulting from chronic inflammation.[4] At the early onset of inflammation, repeated cycles of epithelial mucosal damage and repair resulted in generalized epithelial hyperplasia and developed airway remodeling.[5] Inflammation-, cell apoptosis-, proliferation-, and tissue repair-related genes are involved in these courses.[6,7] All these gene expressions can be affected by microRNAs (miRNAs) due to the ability of any single miRNA to target hundreds of mRNAs, and miRNAs have been considered as potential impact on both the contribution to and protection from COPD.[8] For instance, it has been demonstrated that miR-218-5p,[9] let-7c,[10] miR-1246,[11] miR-145/338,[12] et al, are significantly associated with COPD between the COPD patients and normal volunteers. Meanwhile, several miRNA-mRNA networks have been found to be closely involved in the pathophysiological process of COPD, such as miR-126/ATM (ataxia-telangiectasia mutated) protein kinase,[13] miR-320d/NF-κB,[8] miR-146a-5p/IL-1α,[14] miR-133a/RhoA,[15] miR-542-5p/SMAD2/3.[16]

However, rare studies have focused on the function of miRNA-mRNA networks in epithelial cell proliferation of COPD. In the present study, two GEO databases, which investigated the circulating miRNA expressions (GSE70080) and RNA-sequencing of bronchial epithelial cells (BECs) (GSE130928) between normal subjects and COPD patients, were used to re-analyze and screen out the potential miRNA-mRNA network(s) that influenced the proliferation of BECs. Meanwhile, the anti-proliferative activities of γ-sitosterol (GS) on human BEC lines under inflammatory stimulation were evaluated. γ-sitosterol is a steroidal compound which is first reported by Maurice M. Best in 1954.[17] Then, it is reported that γ-sitosterol could be isolated from L. nodiflora.[18] It is further identified that γ-sitosterol possesses multiple bioactivities and is considered as a powerful anti-inflammatory,[19] anti-diabetic,[20] and anti-tumor agent.[21] However, whether γ-sitosterol has a role of improving COPD has not been studied.

In this study, we attempted to find out the circulating miRNAs, modulated the expressions of BECs hyperplasia-associated genes and investigated whether γ-sitosterol could ameliorate this pathological process via regulating the expressions of COPD-related miRNAs and/or mRNA. We hope the present study can explore new mechanisms of COPD and develop potential drug.

Materials and Methods

Cell Culture and Treatment

Human bronchial epithelial cell lines, HBEpiC, 16HBE, BEP2D, were purchased from Biovector Science Lab, Inc. (Beijing, China). HBE135-E6E7 (CRL-2741), HBEC3-KT (CRL-4051), HBE4-E6/E7 (CRL-2078), A549 (CCL-185) were obtained from American Type Culture Collection (ATCC). BEAS-2B and bronchial carcinoma cells H292 were brought from the China Center for Type Culture Collection (CCTCC, Wuhan University, Wuhan, Hubei province, China). Cells were cultured as respective instructions. Highly pure (>99%) γ-sitosterol (GS) was extracted from Jing-Fang Granule by the State Key Laboratory of Generic Manufacture Technology of Chinese Traditional Medicine (Lunan Pharmaceutical Group Co. Ltd, Linyi, Shan Dong province, China). For in vitro assay, GS was dissolved in dimethyl sulfoxide (DMSO) at a series of concentrations and used to treat cells (from 10^{-4} to 10^{4} μM). GS was used to stimulate the BEAS-2B and H292 cells for 12, 24, 48, and 72 h. Cell proliferation and cell cycle were determined subsequently.

Cell Inhibition, Apoptosis, and Cell Cycle Assays

A CellTiter 96®Aqueous Nonradioactive Cell Proliferation Kit (#TB169, Promega Corporation, Madison, WI, USA) was used to determine the number of viable cells treated with GS. In brief, cells were seeded in 96-well plates at a density of 10^{4} cells/well and cultured for 12 h. Subsequently, cells were treated with GS at different concentrations from 10^{-4} to 10^{4} μM for 24 h. Then, 20 μL MTS/PMS solution was added to each well. After 4 h, absorbance at 490 nm was recorded using Spectramax M2 microplate reader (Molecular Devices, CA, USA). The IC_{50} of GS was calculated using GraphPad prism 5.0 software.

Cell death induced by GS was detected using Annexin V-FITC/propidium iodide (PI) apoptosis detection kit (BD Biosciences, CA, USA) by flow cytometry. Briefly, H292 and BEAS-2B cells were treated with GS for 24 h and then harvested. Staining was performed with 10 μL Annexin V-FITC reagent containing 5 μL PI for 20 min on ice. The cells were then resuspended in 400 μL binding buffer. Fluorescence-activated cell sorter (FACS) analysis was used for analyzing cell apoptosis.

Patients and Ethics Statement

Blood samples were collected from 20 COPD patients and 20 healthy volunteers at the Binzhou Medical University Hospital. The miRNAs in plasma were isolated using the TaqMan® miRNA ABC Purification Kit (Thermo Fisher, OR, USA). According to the manufacturer's instruction, 50 μL plasma was mixed with 100 μL ABC buffer and vortexed for 30 s. The sample was placed on ice and added 80 μL Human Panel Beads. The beads were then hybridized with miRNA at 20°C for 40 min. Subsequently, 100 μL wash buffer was used to wash the sample, and miRNA was eluted by 100 μL elution buffer.

The miRNA was then converted to cDNA and downstream analysis by quantitative real-time PCR (qRT-PCR). The microRNA levels of miR-361-5p and miR-196-5p in plasma were evaluated by qRT-PCR. Small nuclear RNA (snRNA) U6 was used as an endogenous control. Levels of miRNAs were normalized to a reference U6. This study was approved by the Ethics Committee of the Binzhou Medical University Hospital and was carried out in accordance with the Declaration of Helsinki. All the patients and volunteers obtained informed consent for experimentation.

Microarray Analysis

Two Gene Expression Omnibus (GEO) database (https://www.ncbi.nlm.nih.gov/geo/) including circulating miRNA expressions array (GSE70080) and RNA-sequencing of bronchial epithelial cells array (GSE130928) which compared COPD patients with healthy controls were used to re-analyze. Based on the expression matrix, R-limma package was used to compare two groups regarding log2 expression values. The screening criteria were set as $p < 0.05$ and log2 |Fold Change (FC)|>2. Differentially expressed genes were plotted in heatmaps using the online tool Idep.90 database (http://bioinformatics.sdstate.edu/idep/).

Transient Transfection, Luciferase Assay and Immunofluorescence Staining

For cell transfection, micrOFF hsa-miR-196b-5p inhibitor, 5nmol (Cat#, miR20001080-1-5), micrON hsa-miR-196b-5p mimic,5nmol (Cat#, miR10001080-1-5), micrON hsa-miR-361-5p mimic,5nmol (Cat#, miR10000703-1-5), micrOFF hsa-miR-361-5p inhibitor, 5 nmol (Cat#, miR20000703-1-5) were synthesized and purified by RiboBio. Human *bcat1*-3′UTR, *arhgef12*-3′UTR were gifts from Professor Han-yang Hu of Wuhan University. For cell transfection, BEAS-2B and H292 cells were cultured in 6-well plates at a density of 5×10^5 cells per well. When cells grow to approximately 60–70% confluence in antibiotic-free normal growth medium, they are transfected with miRNA mimics, inhibitors, or plasmids for 48 h. For luciferase assays, 15 ng pGL-3-*bcat1*-3′UTR, or pGL-3-*arhgef12*-3′UTR plasmids were, respectively, used to transfect BEAS-2B and H292 cells with or without miRNA (miR-361 and miR-196) mimic/inhibitor. After 48 h, the cells were lysed to determine luciferase activities by the Dual-Glo Luciferase Assay System (Promega). Experiments were performed in triplicate.

Quantitative Real-Time PCR Analysis

To detect mRNA and/or microRNA levels, total RNA in cell lines and miRNA in human plasma were extracted, respectively, according to the manufacturer's instructions. cDNA was synthesized using a cDNA Synthesis Kit (Toyobo, Osaka, Japan) or a Mir-X™ miRNA First Strand Synthesis kit (Takara Bio, Beijing, China). Quantitative real-time PCR (qRT-PCR) was performed using SYBR Green (Toyobo; Osaka, Japan) or a Mir-X™ miRNA RT-qPCR SYBR® kit (cat no. 638314; Takara Bio, Inc.), respectively. The primer sequences for PCR were as follows: has-miR-361, P1 5′-ATAAAGTGCTGACAGTGCAGATAGTG-3′ and P2 5′-TCAAGTACCCACAGTGCGGT-3′; has-miR-196, P1 5′-ATCCTTCCTAGTCCAGCCTGAG-3′ and P2 5′-ACCTGGCGGCACTCCTTA-3′; arhgef12, P1 5′-GGAGCATCTGGGAATATGGA-3′ and P2 5′-TCTTGCAGCTGAGGAATGTG-3′; bcat1, P1 5′-CAACTATGGAGAATGGTCCTAAGCT-3′ and P2 5′-TGTCCAGTCGCTCTCTTCTCTTC −3′; gapdh, P1 5′-GGCGACCTGGAAGTCCAACT3′, and P2, 5′-CCATCAGCACCACAGCCTTC3′; U6, P1 5′-CTCGCTTCGGCAGCACA3′; P2 5′-AACGCTTCACGAATTTGCGT3′. Gapdh was used as internal control for bcat1, arhgef12, and U6 was used as an internal control for miR-361, miR-196.

Immunofluorescence and Immunoblot Assays

To investigate the protein levels including ARHGEF12 (Rabbit anti-ARHGEF12 antibody, Affinity, DF4432), BCAT1 (Rabbit anti-BCAT1, ab197941, Abcam), RhoA (Rabbit Anti-RhoA), ROCK1 (RabbitAnti-ROCK1, ab134181, Abcam), PTEN (Rabbit Anti-PTEN, ab32199, Abcam), mTOR (Rabbit Anti-mTOR, ab134903, Abcam), and pS6K1 (Rabbit Anti-pS6K1, ab32529, Abcam), BEAS-2B cells treated with GS were then transfected

with miRNA. After 48 h, Western Blot was employed to detect protein expression. SDS-PAGE gels electrophoresis was used to separate 20 μg total cell proteins, which were transferred to polyvinylidene difluoride (PVDF) membranes. The membranes were blocked with 5% milk at 4 °C overnight and then incubated with respective primary antibodies at different dilutions (ARHGEF12, 1:1000; BCAT1, 1:500; RhoA, 1:3000; ROCK1, PTEN, mTOR, pS6K1, 1:2000; GAPDH, 1:4500) at RT for 4 h. Afterwards, the membranes were further incubated with horseradish peroxidase (HRP)-conjugated secondary antibody (1:6000, Millipore, Billerica, MA) at RT for 1 hr. After TBST washing, immunoreactive signals were detected using an enhanced chemiluminescence reaction (Thermo Fisher Scientific, Inc.) and recorded by an AutoChemi Imaging System (UVP LLC, CA, USA). The gray value of the bands was analyzed using MCID Elite software (InterFocus Imaging Ltd., Linton, UK).

Statistical Analysis

Values are presented as mean ± S.D. Significant differences among groups were analyzed using a one-way analysis of variance. Specific mean differences were determined by Tukey's test. All statistical analyses were performed using GraphPad Prism software (ver. 4.0; GraphPad, La Jolla, CA, USA). A value of $p < 0.05$ was considered to be significant.

Results

Clinical Characteristics of Subjects

We enrolled 40 cases in total including 20 healthy volunteers and 20 COPD patients without asthma history. The demographic and clinical characteristics are listed in Table S1. It was observed that there were no significant differences in race, gender, age, and body mass index (BMI) between the two groups. Lung function of COPD patients was largely decreased compared with healthy subjects. FEV1/FVC and FEV1 (% predicted) were both lower in patients with COPD than those in healthy subjects.

GS Inhibited Cell Viability, Proliferation, Clone Formation, and Cell Cycle in BEAS-AB Cells, but Not in H292 Cells

To investigate the potential biological activities of GS, H292 and BEAS-2B cells were treated with GS in series concentrations (from 10^{-4} to 10^{4} μM), and cell viabilities were detected and calculated after 24 h stimulation. As results showed in Figure 1A, compared with H292 cells, GS exhibited stronger inhibitory effects on cell viability in BEAS-2B cells: the IC_{50} were 0.22 μM and 0.06 μM in H292 and BEAS-2B cells, respectively. Next, 0.06 μM (60 nM) GS was used to detect time-dependent effects on cell proliferation. In H292 cells, only GS-treatment for 72 h showed significant differences in cell proliferation. In contrast, BEAS-2B cells were more susceptible to GS stimulation (Figure 1B and C, $*p<0.05$). Additionally, colony formation assay demonstrated that 60 nM GS significantly inhibited BEAS-2B cells, but did not inhibit H292 cells (Figure 1D, $*p<0.05$). Subsequently, a flow cytometry assay was performed to further determine whether cell cycle and/or cell apoptosis was mediated by GS-induced inhibitory effects in BEAS-2B cells. As expected, after 60 nM GS was treated for 24 h, neither cell apoptosis (the apoptotic rates were 9.32 ± 1.14% in GS-treatment vs 3.15 ± 1.05% in control. Figure 1E and G) nor cell cycle (Figure 1H and J) were significantly influenced in H292 cells. However, in BEAS-2B cells, GS significantly induced cell apoptosis (the apoptotic rates were 48.75 ± 4.46% in GS-treatment vs 3.01 ± 1.23% in control. Figure 1F and G) and induced G2/M phase arrest (Figure 1I and J, $*p<0.05$). All the data presented indicated that GS blocked BEAS-2B cells in G2/M phase and induced cell apoptosis, which resulted in cell proliferation inhibition, but had no effects on H292 cells.

Distinguished Expressions of miR-196-5p and miR-361-5p Circulating Was Associated with BECs Proliferation of COPD

The circulating miRNA expressions array (GSE70080) which compared COPD patients with healthy controls was downloaded from Gene Expression Omnibus (GEO) database (https://www.ncbi.nlm.nih.gov/geo/). After re-analysis, compared with healthy control, a total of 121 miRNAs (61 up- and 60 down-regulated) were significantly changed in COPD patients (Figure 2A and B). To elucidate the biological function of these miRNAs, enrichment analyses were conducted via the predicted target pathway by using Kyoto Encyclopedia of Genes and Genomes (KEGG) signal pathway analysis on database GSE70080 (Figure S2, Table S2). Among these 121 miRNAs, representative 10 significant differential expression miRNAs are shown in Figure 2B and Table S3. And miR-196-5p, miR-361-5p were top 2 distinguished miRNAs between COPD patients and healthy controls

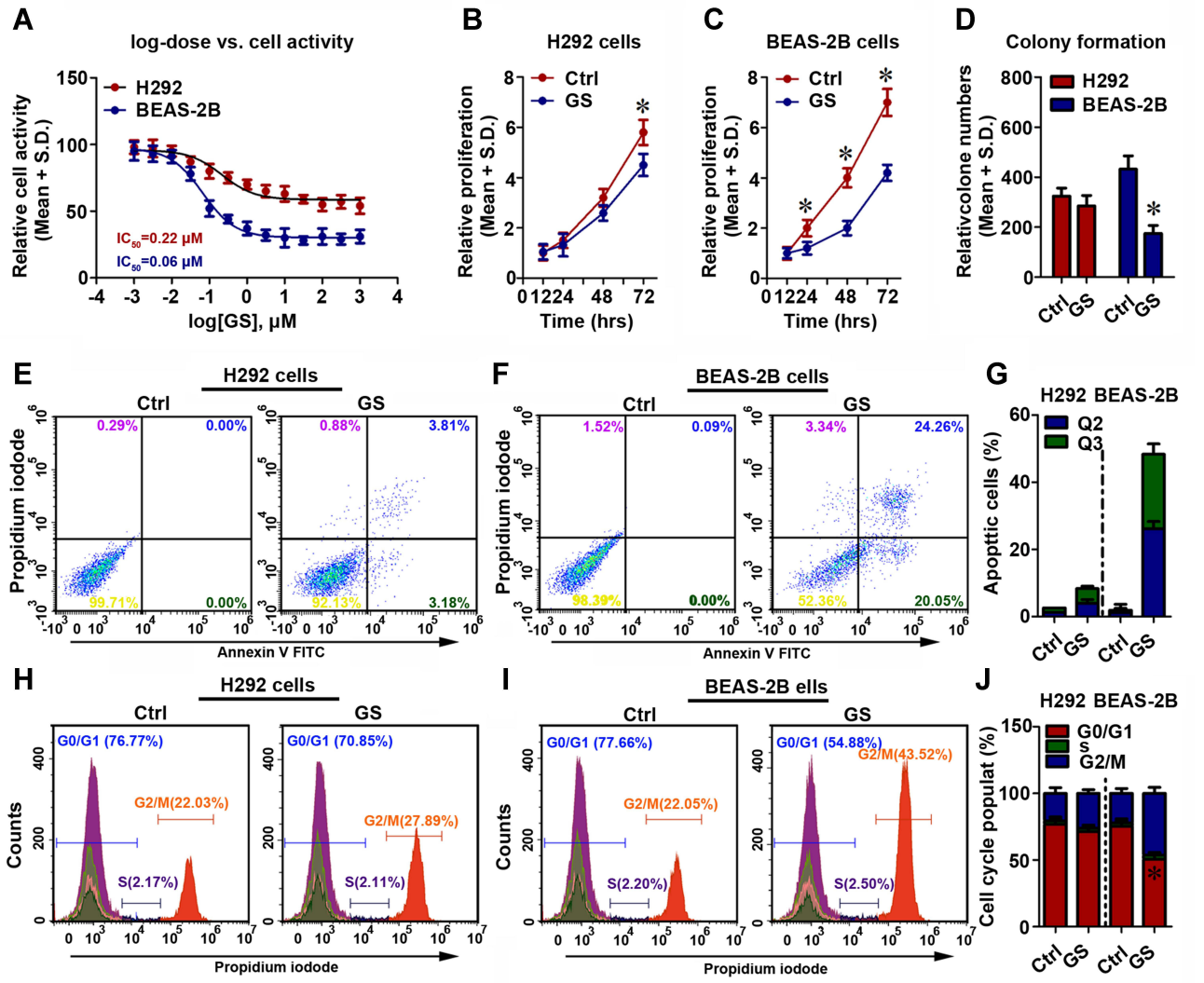

Figure 1 Effect of GS on cell growth and cell cycle. Cell activities of BEAS-2B and H292 cells after treated by GS in series concentrations for 24 h (**A**). Cell proliferation (**B** and **C**), Colony formation (**D**), cell cycles (**E**–**G**), and apoptosis (**H**–**J**) of BEAS-2B, H292 cells after 60 nM GS treatment. Shown are representative and expressed as the means ± SD. The bars with different superscripts in each panel were significantly different. Experiments were performed in triplicate for each group, *p< 0.05.

(Figure 2C, Table S3). Subsequently, the levels of miR-196-5p and miR-361-5p in plasma were detected from 20 COPD patients and 20 healthy volunteers. The results confirmed that, compared with normal control, miR-196-5p and miR-361-5p were, respectively, up- and down-regulated in COPD patients (Figure 2D, *p<0.05). Meanwhile, correlation analysis in COPD patients showed that the circulating miR-196-5p and miR-361-5p were negatively correlated (R^2=0.749, Figure 2E). To further investigate the expression levels of miR-196-5p and miR-361-5p in BECs, HPAEpic, 16HBE, BEAS-2B, BEP2D, HBE135-E6E7, HBEC3-KT, HBE4-E6/E7, A549 and H292 cells, these 9 cell lines were used for miRNA detection. Noticeable results demonstrated that the lowest and highest miR-196-5p were separately H292 and BEAS-2B cells in all nine cell lines. The expression of miR-196-5p was also relatively low in HBE135-E6E7 cell and A549 cell, but relatively high in HBE4-E6/E7 cell and HBEC3-KT cell. In contrast, the miR-361-5p level expressed in BEAS-2B cells is low, but both over-expressed in 16HBE and H292 cells. The expression of miR-361-5p was also low in HBE4-E6/E7 cell and HBEC3-KT cell, but not the lowest (Figure 2F). Based on these above results, BEAS-2B and H292 cells were used as cell models to perform subsequent experiments. The miRNA mimics and inhibitors of both miR-196-5p and miR-361-5p were, respectively, transfected into BEAS-2B and H292 cells, the cell proliferation was detected and the results are showed in Figure 2G and H, *p<0.05. Over-expressed miR-196-5p and inhibited miR-

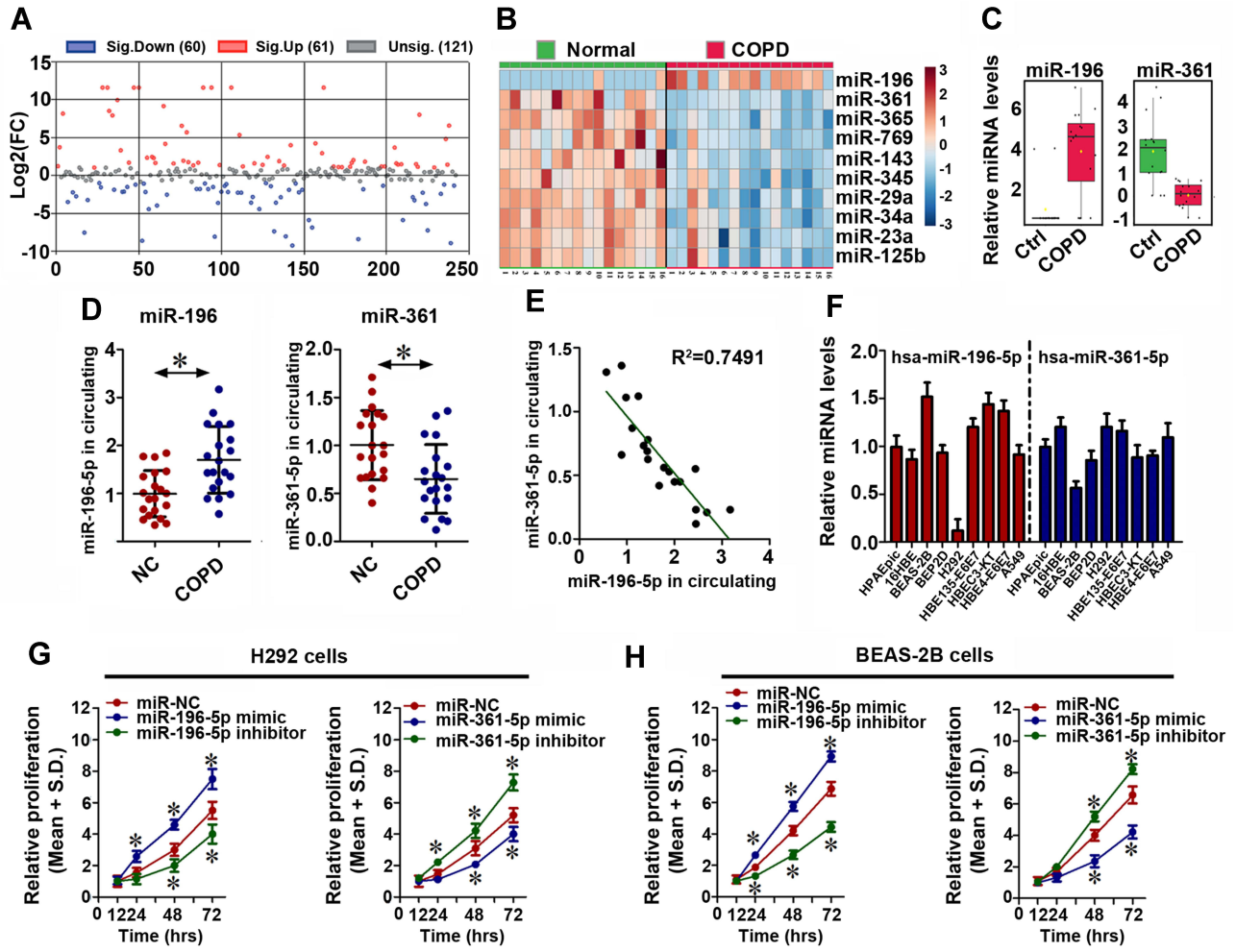

Figure 2 Effect of miR-196-5p and miR-361-5p expression on BECs proliferation. 121 significantly changed miRNAs (**A**), and top 10 miRNAs (**B** and **C**) were screened out from GSE70080. The expression levels of miR-196-5p and miR-361-5p were detected from 20 COPD and 20 healthy volunteers (**D** and **E**), and five human BEC lines (**F**). Cell proliferations were performed in H292 (**G**) BEAS-2B (**H**) cells after miRNA mimics or inhibitors stimulation. Shown are representative and expressed as the Means ± S. D. The bars with different superscripts in each panel were significantly different. Experiments were performed in triplicate for each group, *p< 0.05.

361-5p were significantly associated with cell proliferation in both BEAS-2B and H292 cells. Alternatively, suppressing miR-196-5p or promoting miR-361-5p level robustly decreased cell proliferation rates. However, compared with H292, BEAS-2B cells proliferation proved to be more sensitive when the cells were subjected to the same treatment. Together, the above results demonstrated that up-regulated miR-196-5p and down-regulated miR-361-5p may be involved in COPD patients BECs proliferation.

GS Regulated miR-196-5p and miR-361-5p Expressions in BEAS-2B Cells, but Not in H292 Cells

In retrospect, from the results in Figure 1, GS showed more effective biological activity in BEAS-2B, but not in H292 cells. Due to a distinguishing expression of miR-196-5p and miR-361-5p in BEAS-2B and H292 cells, we speculate that miR-196-5p and miR-361-5p may be involved in GS-induced inhibition in cell proliferation. Therefore, the expression levels of miR-196-5p and miR-361-5p were detected after 60 nM GS treatment for 24 h in H292 and BEAS-2B cells. Interestingly, although GS significantly suppressed miR-196-5p and promoted miR-361-5p levels in BEAS-2B cells, respectively, this regulatory function was invalid in H292 cells (Figure 3A, *p<0.05). To further investigate whether miR-196-5p and/or miR-361-5p are necessary for GS biological activity, miR-196-5p mimic and miR-361-5p inhibitor were used to treat BEAS-2B cells with or without GS. The results showed that either miR-196-5p mimic or miR-361-5p inhibitor could significantly promote cell proliferation, which neutralized GS-induced inhibitory effects

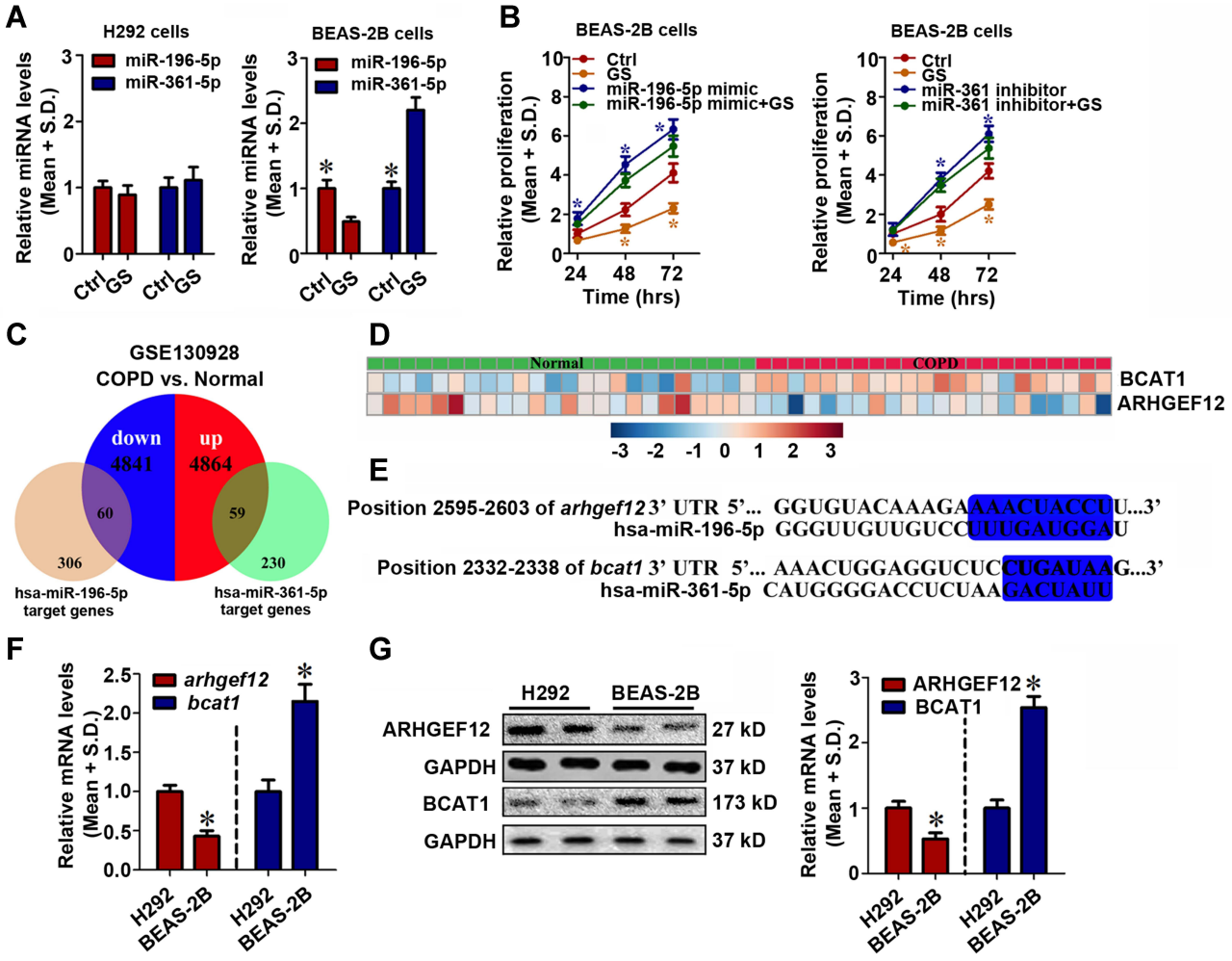

Figure 3 Effect of GS on regulating miR-196-5p and miR-361-5p expression. (**A**) After GS treatment, the expressions of miR-196-5p and miR-361-5p were detected in BEAS-2B and H292 cells. (**B**) Cell proliferation were performed in BEAS-2B cells after GS single or combined with either miR-196-5p mimic or miR-361-5p inhibitor. (**C**) miR-196-5p and miR-361-5p target mRNAs were matched to GSE130928 profile, respectively. The expressions of bcat1 and arhgef12 of GSE130928 were showed in (**D**) and the binding motifs of miR-196-5p to arhgef12 and miR-361-5p to bcat1 were showed in (**E**), respectively. The mRNA (**F**) and protein levels (**G**) were detected in H292 and BEAS-2B cells. Shown are representative and expressed as the Means ± S.D. The bars with different superscripts in each panel were significantly different. Experiments were performed in triplicate for each group, *$p< 0.05$.

(Figure 3B, *$p<0.05$). The above results confirmed that miR-196-5p and miR-361-5p are functional for cell proliferation and simultaneously regulated by GS.

Arhgef12 and Bcat1 Were Respective Potential Targets of miR-196-5p and miR-361-5p in BECs

Next, it is necessary to search for the target proteins of miR-196-5p and miR-361-5p and investigate the signal pathways involved in BECs proliferation in COPD. Therefore, another RNA-sequencing of bronchial epithelial cells array (GSE130928) which compared COPD patients with normal volunteers was used to re-analyze. Meanwhile, miR-196-5p and miR-361-5p target genes were predicted by TargetScan (www.targetscan.org/) and miRBase (www.mirbase.org/) online websites. After analysis, 4901 down- and 4923 up-regulated genes were screened out from GSE130928 (COPD vs Ctrl). Meanwhile, 366 miR-196-5p target genes and 289 miR-31-5p target genes were predicted. After screening, 60 and 59 candidate genes were obtained after matching miR-196-5p target genes to 4901 down-regulated genes in GSE130928 and matching miR-361-5p to 4923 up-regulated genes in GSE130928, respectively (Figure 3C). Subsequently, two of the most significantly distinguished genes, BCAT1 (over-expressed in COPD BECs vs normal control) and ARHEGF12 (suppressed in COPD BECs vs normal control) were selected as candidate targets of miR-361-5p and miR-196-5p, respectively (Figure 3D). The

predicted binding sites are showed in Figure 3E. The mRNA and protein levels of BCAT1 and ARHGEF12 were detected in H292 and BEAS-2B cells. Compared with H292, both expression level of BCAT1 and ARHGEF12 were more different in BEAS-2B cells. RNA and protein levels of ARHGEF12 were low in BEAS-2B cells; however, RNA and protein levels of BCAT1 were high in this cell line (Figure 3F and G, *p<0.05).

miR-196-5p/arhgef 12 and miR-361-5p/bcat1 Pathways Mediated GS-Induced Anti-Proliferative Effects on BECs

To further investigate whether miR-196-5p and miR-361-5p are separately functional for arhgef 12 and bcat1 expression, H292 and BEAS-2B cells were transfected with luciferase-*arhgef 12* 3′URT or *bcat1*3′URT plasmid. The luciferase activities were detected after cells were treated with either miR-196-5p mimic (or inhibitor) or miR-361-5p mimics (or inhibitor). As shown in Figure 4A, *p<0.05, the luciferase activity of *arhgef 12* 3′URT in both H292 and BEAS-2B cells significantly decreased after miR-196-5p mimic-treatment, but was dramatically raised by miR-196-5p inhibitor. Meanwhile, the luciferase activity of *bcat1* 3′URT has the same trend under either miR-361-5p mimic or inhibitor treatment (Figure 4B, *p<0.05). Subsequently, the effects of GS on *arhgef 12* 3′URT or *bcat1* 3′URT luciferase activities were evaluated in H292 and BEAS-2B cells. Inevitably, neither *arhgef 12* 3′URT nor *bcat1*3′URT was influenced in GS-treated H292 cells (Figure 4C). However, GS promoted *arhgef 12* 3′URT and suppressed *bcat1* 3′URT luciferase activities in BEAS-2B cells. These effects were ameliorated when BEAS-2B cell was treated by GS combined with either miR-196-5p mimic or miR-361-5p inhibitor (Figure 4D, *p<0.05). In addition, mRNA and protein levels of ARHGEF 12 and BCAT1 were also detected in BEAS-2B cells under GS and miRNA treatment. Both mRNA and protein expressions of ARHGEF12 were induced by GS, but suppressed by miR-196-5p mimic single or combined with GS. In contrast, BCAT1 mRNA and protein levels were down-regulated by GS and reversely elevated in BEAS-2B when cells were subjected to miR-361-5p inhibitor treatment or miR-361-5p inhibitor combined with GS treatment (Figure 4E–G, all p<0.05). Meanwhile, cell immunofluorescence assay also further verified the above results (Figure 4H). Subsequently, the expression levels of proteins involved in ARHGEF 12 (eg GTP-RhoA, ROCK1, PETN) and BCAT1 (eg mTOR, pS6K1) related pathways were detected by Western blots. As results showed in Figure 4I, compared with control group, GS could elevate GTP-RhoA protein expression level but miR-196-5p mimic decreased this protein expression, and miR-196-5p mimic reversed the GS function. However, the total RhoA expression was not changed, indicating that either GS or miR-196-5p mimic only regulates RhoA activity, but not RhoA expression. As a consequence, GS efficiently upregulated the expression of ROCK1 and PTEN, but suppressed the expression of mTOR protein. However, miR-196-5p mimic significantly inhibited the expression of ROCK1 and PTEN and promoted mTOR expression. Additionally, miR-361-5p inhibitor remarkablely raised mTOR and pS6K1 expression levels and eliminated GS-induced inhibitory effects on protein expressions (Figure 4J). Protein quantitative results are shown in Figure 4K and L.

Together, all the results above confirmed that, under physiological condition, relatively more miR-361-5p targeting *bact1* 3′UTR and less miR-196-5p targeting *arhgef12* 3′UTR in BECs resulted in low BCAT1 and high ARHGEF12 protein expressions. In one way, as an enzyme metabolizing Branched-chain α-keto acids (BCKAs) into branched-chain amino acids (BCAAs), low-expressed BCAT1 decreased BCAAS production, merely partially activated mTOR-pS6K pathway and slightly promoted BECs proliferation. In another way, high expressed ARHGEF12 protein could activate RhoA and subsequently promote ROCK and PTEN expressions, then later inhibite mTOR-pS6K pathway, resulting in anti-proliferation of BECs. In contrast, under COPD condition, the levels of miR-361-5p and miR-196-5p are reversed, causing enhanced BCAAS-mTOR-pS6K and weakened RhoA-ROCK-PTEN pathway and resulting in BECs proliferation. GS could simultaneously inhibit miR-196-5p and promote miR-361-5p levels, then ameliorate mTOR-pS6K pathway, and finally exert an anti-proliferation function on BECs in COPD (Figure 5). This is a potential mechanism for GS exerting biological activity.

Discussion

The homeostasis between apoptosis and proliferation of BECs is vital for maintaining the normal physiological functions of the lung.[22] Damage-repair of BECs together form a vicious cycle and excessive repairment finally results in generalized epithelial hyperplasia, which eventually develops into squamous metaplasia, a reversible replacement of

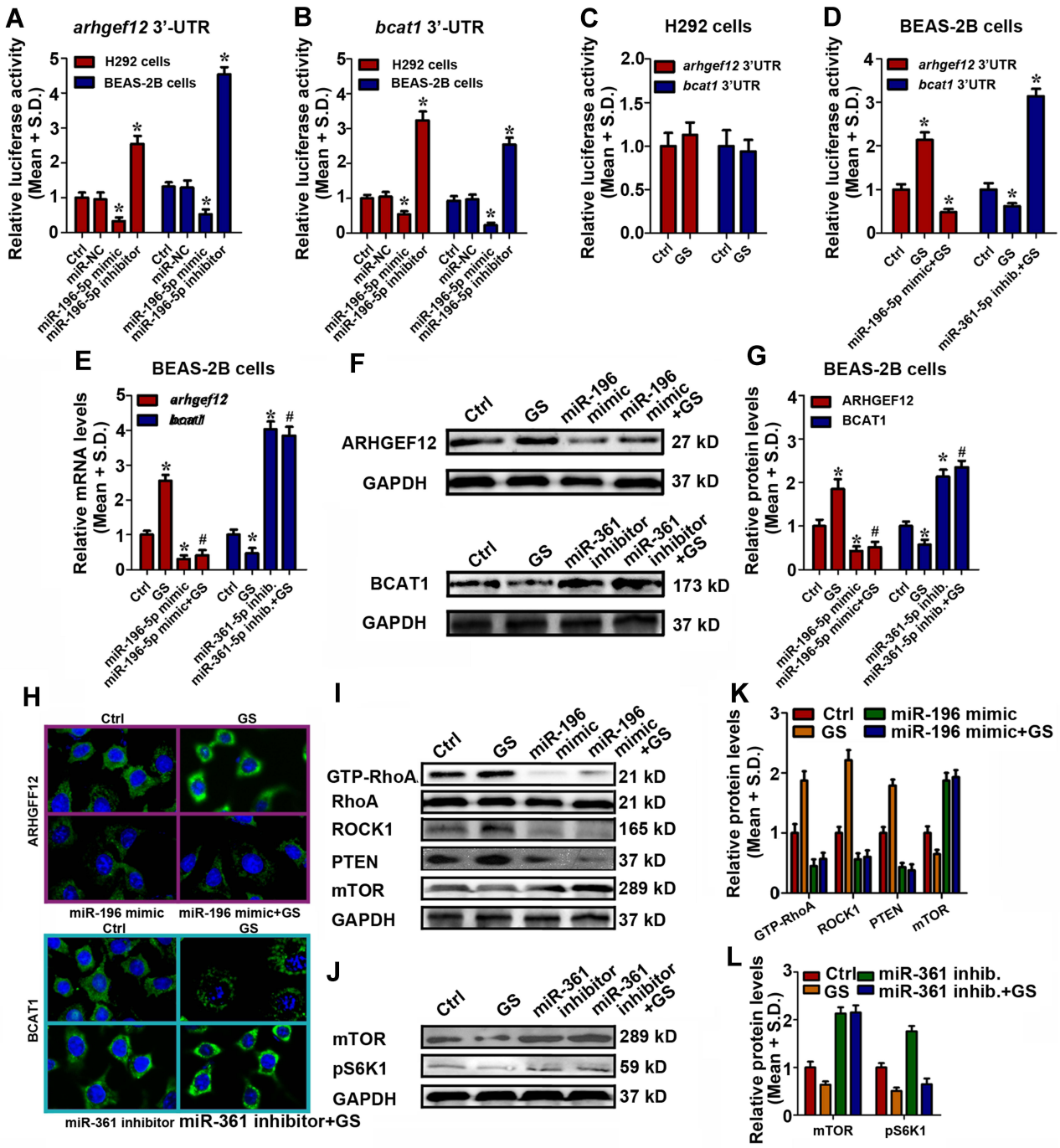

Figure 4 miR-196-5p/arhgef 12 and miR-361-5p/bcat1 pathways involved in GS-induced anti-proliferative effects on BECs. The luciferase assay were performed in H292 and BEAS-2B cells after pGL-3-*bcat1*-3'UTR and pGL-3-*arhgef12*-3'UTR plasmids co-transfected with specific miRNA mimics or inhibitors (**A** and **B**), or stimulated by GS with or without miR-195-5p mimic (or miR-361-5p inhibitor) (**C** and **D**). The mRNA (**E**), protein (**F** and **G**), and immunofluorescence (**H**) levels of ARHGEF12 and BCAT1 were detected in BEAS-2B cells after stimulated by GS with or without miR-195-5p mimic or miR-361-5p inhibitor. (**I** and **J**) The protein levels of GTP-RhoA, RhoA, ROCK1, PTEN, mTOR, and pS6K1 were detected in BEAS-2B cells after stimulated by GS with or without miR-195-5p mimic or miR-361-5p inhibitor. (**K** and **L**) Shown are representative and expressed as the Means ± S.D. The bars with different superscripts in each panel were significantly different. Experiments were performed in triplicate for each group, **p*< 0.05 vs Control, #*p*<0.05 vs GS.

normal ciliated respiratory epithelium by squamous epithelium.[23] Inhibition of excessive proliferative BECs is beneficial to the remission or treatment of COPD. In the present study, anti-proliferation effect of γ-sitosterol (GS) was evaluated in BEAS-2B and H292 cells. The results showed that, in BEAS-2B cells, GS exerted well anti-proliferative effects including inhibiting cell activity, proliferation, colony formation, modulating cell cycle arrested in

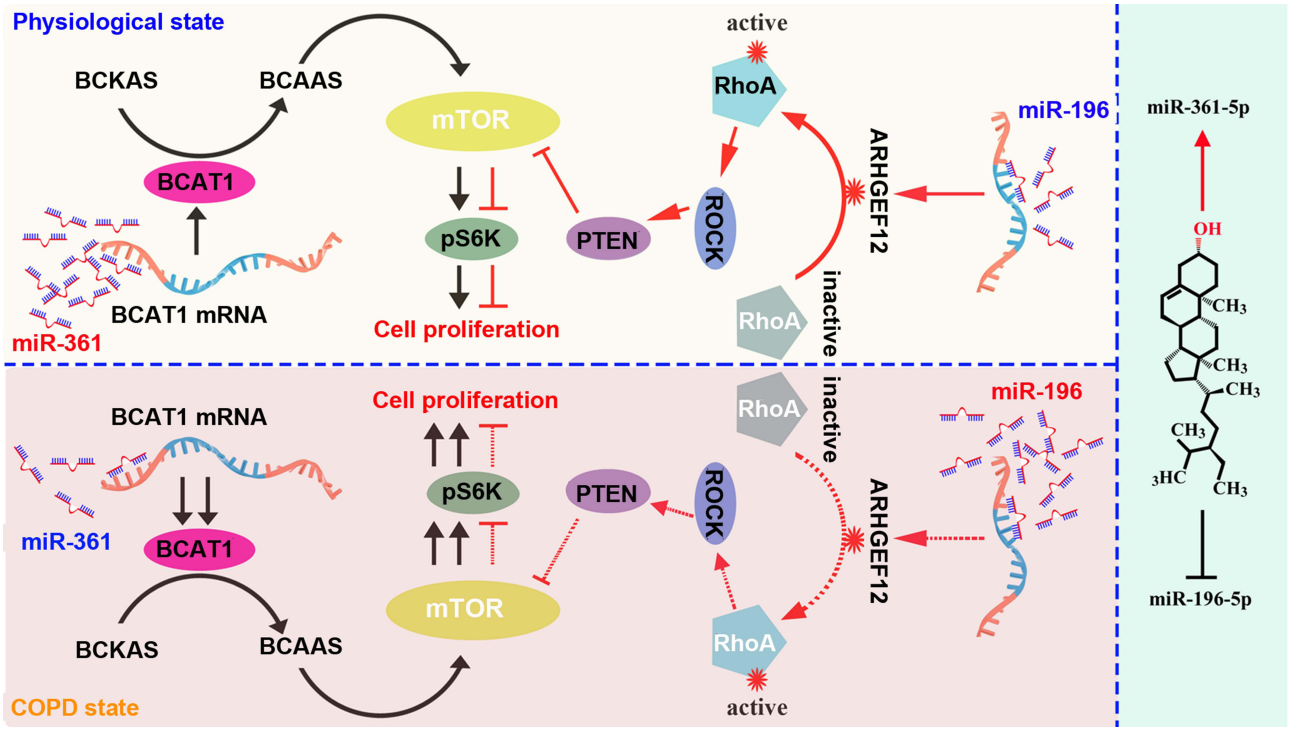

Figure 5 Potential mechanism of GS exerting biological activity. Under physiological condition, relatively more miR-361-5p and less miR-196-5p in BECs respective targeting *bact1* and *arhgef12* 3′UTR result to low BCAT1 and high ARHGEF12 protein expressions. In one way, as an enzyme metabolizing BCKAS to BCAAS, low expressed BCAT1 decrease BCAAS production, which merely partial activate mTOR-pS6K pathway and slightly promoting BECs proliferation. In another way, high expressed ARHGEF12 protein activate and subsequently promote ROCK and PTEN expressions, the later inhibit mTOR-pS6K pathway and result to anti-proliferation of BECs. In contrast, under COPD condition, the levels of miR-361-5p and miR-196-5p are reversed, which cause enhanced BCAAS-mTOR-pS6K and weakened RhoA-ROCK-PTEN pathway result to BECs proliferation. The biological activities of GS are simultaneously inhibits miR-196-5p and promote miR-361-5p levels in order to ameliorate mTOR-pS6K pathway, finally exert anti-proliferation of BECs in COPD.

G2/M phase and inducing cell apoptosis. Interestingly, the above biological activities were not observed in H292 cells (Figure 1). As a well-known anti-inflammatory agent, wide studies have demonstrated that GS possessed multiple bioactivities including anti-diabetes,[21] modulating cell cycle and inducing apoptosis of breast and lung cancer cells.[20] *Nepeta cataria L* and *Saposhnikovia divaricata (Trucz.) Schischk* were reported containing abundant GS[24,25] and widely applied for spasmolytic and bronchodilatory,[26] anti-inflammatory, antipyretic, and analgesic agent.[27] Jing Fang granules, an over-the-counter prescription for traditional Chinese medicine produced by Lunan Pharmaceutical Group containing *Nepeta cataria L.*, and *Saposhnikovia divaricata (Trucz.) Schischk.*, is used to treat cough, nasal obstruction, headache, pain, cold aversion and no sweat in clinical. We used Thermo Fisher Vanquish UHPLC instrument to detect the components of Jing Fang granules and analyzed the components using the Thermo Fisher Q Exactive Mass Spectrometer assay (Thermo Fisher Scientific, Shanghai, China). The results confirm that GS is one of the most abundant components (Figure S1).

Until now, it has been emergent to find out biomarkers and potential therapeutic targets for COPD. miRNAs were considered as potential therapeutic targets due to the fact that a single miRNA could regulate a dozen even hundreds of mRNA expressions.[28,29] However, no previous studies have focused on the effects of circulating miRNAs on BECs proliferation in COPD. In the present study, a GSE data (GSE70080) that compared circulating miRNAs of COPD patients with healthy donors was used to re-analyze and two of the most significantly changed miRNAs, miR-196-5p and miR-361-5p were screened out. As data showed, compared with healthy volunteers, miR-196-5p and miR-361-5p in serum of COPD patients were, respectively, up- and down-regulated. And the result was confirmed by the following comparison between 20 normal controls and COPD patients (Figure 2A–E). On the basis that miR-196-5p was increased and miR-361-5p was decreased in COPD patients compared with healthy subjects. We further intended to screen out an epithelium cell line with a similar microRNA expression level and used this specific cell line to elucidate the function

of miR-196-5p and miR-361-5p in GS' potential protective role in COPD. We detected the expression of miR-196-5p and miR-361-5p in 9 cell lines including HPAEpic, 16HBE, BEAS-2B, BEP2D, H292, HBE135-E6E7, HBEC3-KT, HBE4-E6/E7 and A549 in the preliminary experiment. It was found that, in BEAS-2B cells, both of these two micoRNA have a consistent change trend with COPD patients. H292 cell was used as a control because these two microRNAs have opposite expression trends in the cell. Actually, the expression of miR-196-5p and miR-361-5p in HBE4-E6/E7 and HBEC3-KT showed a similar level compared to BEAS-2B (Figure 2F), but it is not the most significant. Here, we chose BEAS-2B in the next work for another reason. Although protein phosphatase 2A (PP2A) was inhibited in BEAS2B cells due to SV40 t antigen, it has been identified that a diminished activity of PP2A, a regulator of the inflammatory response in the airways, has been demonstrated in COPD.[30] So, BEAS-2B cell line, as a bronchial epithelium cell line with PP2A inhibition, can mimic COPD primary cells and is the most appropriate choice in the absence of human primary cells. However, H292 cell line is derived from pulmonary mucoepidermoid carcinoma and used for a control. Therefore, BEAS-2B (characterized as high miR-196-5p and low miR-361-5p levels) and H292 (contrary to BEAS-2B with low miR-196-5p and high miR-361-5p levels) were selected for subsequent study and the results demonstrated that over-expressed miR-196-5p and suppressed miR-361-5p could promote cell proliferation in both BEAS-2B and H292 cells (Figure 2F–H). To further investigate the possible roles of miR-196-5p and miR-361-5p on BECs proliferation, miR-196-5p and miR-361-5p were used to treat BEAS-2B and H292 cell lines. Subsequently, whether these two miRNAs mediate the inhibitory effect of GS on BECs proliferation was investigated and the results showed that GS displayed no activity on H292 cells. Meanwhile, in BEAS-2B cells, miR-196-5p and miR-361-5p were regulated by GS (GS significantly suppressed miR-196-5p and promoted miR-361-5p expressions) and finally resulted in anti-proliferation (Figure 3A and B). And KEGG pathway enrichment analysis identified those that were indeed involved in the apoptosis signaling pathway (Table S2). However, the function of GS and the expression level of miR-196-5p and miR-361-5p in human primary airway epithelial cells were still ambiguous; therefore, we will further explore the expression of miR-196-5p and miR-361-5p and GS function in human primary airway epithelial cells in the future work.

As we know, miRNAs perform their biological functions by regulating the expression of target genes.[9] Therefore, after analysis of another RNA-sequencing of bronchial epithelial cells array (GSE130928), two distinguish expressed genes *bcat1* (over-expressed in COPD vs non-COPD) and *arhgef12* (low-expressed in COPD vs non-COPD) were screened out. Meanwhile, both mRNA and protein levels of BCAT1 and ARHGEF12 are negatively correlated with the expressions of miR-196-5p and miR-361-5p in BEAS-2B cells, respectively (Figure 3C–G, Figure 4A and B). However, there were no studies focused on the functions of BCAT1 and ARHGEF12 in COPD. As previous research has indicated, BCAT1 are closely related to cancer and acute myocardial infarction.[31] Activated BCAT1 promotes cell proliferation in nasopharyngeal carcinoma and gliomas,[32–34] and decreases the sensitivity of cancer cells to cisplatin.[35] Meanwhile, BCAT1 is the predominant BCAT isoform in human primary macrophages and BCAT1 inhibition results in decreased oxygen consumption and glycolysis and contributes to a less proinflammatory transcriptome signature.[36] In another way, ARHGEF12 is associated with cancer cell proliferation.[37,38] Low-expression ARHGEF12 is observed in hypoxia-treated pulmonary artery smooth muscle cells and is associated with cell proliferation and migration.[39] There are signs that raised BCAT1 and decreased ARHGEF12 are simultaneously positively correlated with cell proliferation. We therefore presume that miR-361-5p/*ABCA1* and miR-196-5p/*ARHGEF12* axis mediate GS induced anti-proliferation in BECs. We suspect that, in BEAS-2B cells, GS significantly promoted *arhgef12* and suppressed *abca1* in 3′UTR luciferase activities, mRNA, and protein expression levels, which were contrary to the function of miR-196-5p mimic and miR-361-5p inhibitor. However, these effects were not observed in H292 cells (Figure 4C–H). Furthermore, we found that RhoA-ROCK1 pathway was activated and PTEN expression was subsequently increased following elevated ARHGEF12 and decreased ABCA1 expressions induced by GS, which finally resulted in mTOR and BEAS-2B proliferation inhibition (Figure 4I–L). ARHGEF12 is selective for RhoA subfamily GTPases and is an essential regulator of cell migration and invasion. As a key component of RhoA signaling, ARHGEF12 is involved in promoting cell proliferation in some tumor cells, such as Hela, and glioblastoma cell. However, activated RhoA/ROCK1/PTEN pathway would inhibit cell proliferation in some human leukemia cells.[40,41] Here in this study, as shown in

Figure 5, expression of miR-196-5p weakened RhoA-ROCK-PTEN pathway by targeting ARHGEF12 and resulted in BECs proliferation.

Some limitations of the present study should be taken into consideration. First, we only detected the function of GS and the expression of miR-196-5p and miR-361-5p in BECs cell line but not in human primary airway epithelial cells. Second, obtaining data on COPD patients' lung tissue could be helpful in gaining a comprehensive understanding of the role of micro miR-196-5p and miR-361-5p, but we could not get the information on patients' lung samples under current conditions. Finally, we did not perform in vivo experiments. We plan to perform research on the role of miR-196-5p and miR-361-5p in anti-proliferative effects of GS on COPD to overcome these limitations in the future.

Conclusion

Taken together, the present study has demonstrated that the homeostasis between apoptosis and proliferation of BECs is disrupted in COPD state. In COPD patients, it shows that decreased ARHGEF12 expression is dominated by over-expressed miR-196-5p and the elevated level of BCAT1 is due to decreased miR-361-5p. All these imbalances further enhance BCAAS-mTOR-pS6K pathway and inhibit RhoA-ROCK-PTEN pathway, which finally result in BECs proliferation. As an activator of miR-361-5p and inhibitor of miR-196-5p, GS could simultaneously inhibit BECs proliferation in both pathways. These studies exhibit that GS has a very broad application for the COPD treatment in the future (Figure 5).

Ethics Approval and Informed Consent

This study was approved by the Ethics Committee of the Binzhou Medical University Hospital and was carried out in accordance with the Declaration of Helsinki. All participants were informed about the study, and written informed consent was obtained.

Acknowledgments

We wish to thank Dr. HY Hu (University of Wuhan) for kindly providing pGL-3-*bcat1*-3′UTR, or pGL-3-*arhgef12*-3′UTR plasmids.

Disclosure

The authors report no conflicts of interest in this work.

References

1. Vaz M, Hwang SY, Kagiampakis I, et al. Chronic cigarette smoke-induced epigenomic changes precede sensitization of bronchial epithelial cells to single-step transformation by KRAS mutations. *Cancer Cell*. 2017;32(3):360–376 e6. doi:10.1016/j.ccell.2017.08.006
2. Steiling K, van den Berge M, Hijazi K, et al. A dynamic bronchial airway gene expression signature of chronic obstructive pulmonary disease and lung function impairment. *Am J Respir Crit Care Med*. 2013;187(9):933–942. doi:10.1164/rccm.201208-1449OC
3. Ouadah Y, Rojas ER, Riordan DP, Capostagno S, Kuo CS, Krasnow MA. Rare pulmonary cells are stem cells regulated by Rb, p53, and notch. *Cell*. 2019;179(2):403–416e23. doi:10.1016/j.cell.2019.09.010
4. Ghebre MA, Pang PH, Diver S, et al. Biological exacerbation clusters demonstrate asthma and chronic obstructive pulmonary disease overlap with distinct mediator and microbiome profiles. *J Allergy Clin Immunol*. 2018;141(6):2027–2036 e12. doi:10.1016/j.jaci.2018.04.013
5. Jing Y, Gimenes JA, Mishra R, et al. NOTCH3 contributes to rhinovirus-induced goblet cell hyperplasia in COPD airway epithelial cells. *Thorax*. 2019;74(1):18–32. doi:10.1136/thoraxjnl-2017-210593
6. Wilkinson T. Understanding disease mechanisms at the nanoscale: endothelial apoptosis and microparticles in COPD. *Thorax*. 2016;71(12):1078–1079. doi:10.1136/thoraxjnl-2016-208993
7. Skronska-Wasek W, Mutze K, Baarsma HA, et al. Reduced frizzled receptor 4 expression prevents WNT/beta-catenin-driven alveolar lung repair in chronic obstructive pulmonary disease. *Am J Respir Crit Care Med*. 2017;196(2):172–185. doi:10.1164/rccm.201605-0904OC
8. Faiz A, Steiling K, Roffel MP, et al. Effect of long-term corticosteroid treatment on microRNA and gene-expression profiles in COPD. *Eur Respir J*. 2019;53(4):1801202. doi:10.1183/13993003.01202-2018
9. Conickx G, Mestdagh P, Avila Cobos F, et al. MicroRNA profiling reveals a role for MicroRNA-218-5p in the pathogenesis of chronic obstructive pulmonary disease. *Am J Respir Crit Care Med*. 2017;195(1):43–56. doi:10.1164/rccm.201506-1182OC
10. Van Pottelberge GR, Mestdagh P, Bracke KR, et al. MicroRNA expression in induced sputum of smokers and patients with chronic obstructive pulmonary disease. *Am J Respir Crit Care Med*. 2011;183(7):898–906. doi:10.1164/rccm.201002-0304OC
11. Cazorla-Rivero S, Mura-Escorche G, Gonzalvo-Hernandez F, Mayato D, Cordoba-Lanus E, Casanova C. Circulating miR-1246 in the progression of chronic obstructive pulmonary disease (COPD) in patients from the BODE cohort. *Int J Chron Obstruct Pulmon Dis*. 2020;15:2727–2737. doi:10.2147/COPD.S271864
12. Lacedonia D, Palladino GP, Foschino-Barbaro MP, Scioscia G, Carpagnano GE. Expression profiling of miRNA-145 and miRNA-338 in serum and sputum of patients with COPD, asthma, and asthma-COPD overlap syndrome phenotype. *Int J Chron Obstruct Pulmon Dis*. 2017;12:1811–1817. doi:10.2147/COPD.S130616
13. Paschalaki KE, Zampetaki A, Baker JR, et al. Downregulation of MicroRNA-126 augments DNA damage response in cigarette smokers and patients with chronic obstructive pulmonary disease. *Am J Respir Crit Care Med*. 2018;197(5):665–668. doi:10.1164/rccm.201706-1304LE
14. Osei ET, Florez-Sampedro L, Tasena H, et al. miR-146a-5p plays an essential role in the aberrant epithelial-fibroblast cross-talk in COPD. *Eur Respir J*. 2017;49(5):1602538. doi:10.1183/13993003.02538-2016
15. Shigemura M, Lecuona E, Angulo M, et al. Hypercapnia increases airway smooth muscle contractility via caspase-7-mediated miR-133a-RhoA signaling. *Sci Transl Med*. 2018;10(457):eaat1662. doi:10.1126/scitranslmed.aat1662

16. Garros RF, Paul R, Connolly M, et al. MicroRNA-542 promotes mitochondrial dysfunction and SMAD activity and is elevated in intensive care unit-acquired weakness. *Am J Respir Crit Care Med*. 2017;196(11):1422–1433. doi:10.1164/rccm.201701-0101OC
17. Best MM, Duncan CH, Van Loon EJ, Wathen JD. Lowering of serum cholesterol by the administration of a plant sterol. *Circulation*. 1954;10(2):201–206. doi:10.1161/01.cir.10.2.201
18. Balamurugan R, Duraipandiyan V, Ignacimuthu S. Antidiabetic activity of gamma-sitosterol isolated from Lippia nodiflora L. in streptozotocin induced diabetic rats. *Eur J Pharmacol*. 2011;667(1–3):410–418. doi:10.1016/j.ejphar.2011.05.025
19. Adnan M, Nazim Uddin Chy M, Mostafa Kamal ATM, et al. Evaluation of anti-nociceptive and anti-inflammatory activities of the methanol extract of Holigarna caustica (Dennst.) Oken leaves. *J Ethnopharmacol*. 2019;236:401–411. doi:10.1016/j.jep.2019.01.025
20. Sundarraj S, Thangam R, Sreevani V, et al. Gamma-sitosterol from Acacia nilotica L. induces G2/M cell cycle arrest and apoptosis through c-Myc suppression in MCF-7 and A549 cells. *J Ethnopharmacol*. 2012;141(3):803–809. doi:10.1016/j.jep.2012.03.014
21. Balamurugan R, Stalin A, Ignacimuthu S. Molecular docking of gamma-sitosterol with some targets related to diabetes. *Eur J Med Chem*. 2012;47(1):38–43. doi:10.1016/j.ejmech.2011.10.007
22. Lee W, Thomas PS. Oxidative stress in COPD and its measurement through exhaled breath condensate. *Clin Transl Sci*. 2009;2(2):150–155. doi:10.1111/j.1752-8062.2009.00093.x
23. Puchelle E, Zahm JM, Tournier JM, Coraux C. Airway epithelial repair, regeneration, and remodeling after injury in chronic obstructive pulmonary disease. *Proc Am Thorac Soc*. 2006;3(8):726–733. doi:10.1513/pats.200605-126SF
24. Klimek B, Modnicki D. Terpenoids and sterols from Nepeta cataria L. var. citriodora (Lamiaceae). *Acta Pol Pharm*. 2005;62(3):231–235.
25. Chang F, Yu D, Wang H, et al. Authentication of Saposhnikovia divaricata (Trucz.) Schischk and its two adulterants based on their macroscopic morphology and microscopic characteristics. *Microsc Res Tech*. 2021;84(5):1089–1094. doi:10.1002/jemt.23651
26. Gilani AH, Shah AJ, Zubair A, et al. Chemical composition and mechanisms underlying the spasmolytic and bronchodilatory properties of the essential oil of Nepeta cataria L. *J Ethnopharmacol*. 2009;121(3):405–411. doi:10.1016/j.jep.2008.11.004
27. Fu J, Zeng Z, Zhang L, Wang Y, Li P. 4′-O-beta-D-glucosyl-5-O-methylvisamminol ameliorates imiquimod-induced psoriasis-like dermatitis and inhibits inflammatory cytokines production by suppressing the NF-kappaB and MAPK signaling pathways. *Braz J Med Biol Res*. 2020;53(12):e10109. doi:10.1590/1414-431X202010109
28. Rodrigo-Munoz JM, Rial MJ, Sastre B, et al. Circulating miRNAs as diagnostic tool for discrimination of respiratory disease: asthma, asthma-chronic obstructive pulmonary disease (COPD) overlap and COPD. *Allergy*. 2019;74(12):2491–2494. doi:10.1111/all.13916
29. Liu PF, Yan P, Zhao DH, et al. The effect of environmental factors on the differential expression of miRNAs in patients with chronic obstructive pulmonary disease: a Pilot Clinical Study. *Int J Chron Obstruct Pulmon Dis*. 2018;13:741–751. doi:10.2147/COPD.S156865
30. Doherty DF, Nath S, Poon J, et al. Protein phosphatase 2A reduces cigarette smoke-induced cathepsin S and loss of lung function. *Am J Respir Crit Care Med*. 2019;200(1):51–62. doi:10.1164/rccm.201808-1518OC.
31. Lai Q, Yuan G, Shen L, et al. Oxoeicosanoid receptor inhibition alleviates acute myocardial infarction through activation of BCAT1. *Basic Res Cardiol*. 2021;116(1):3. doi:10.1007/s00395-021-00844-0
32. Liu R, Liu J, Wu P, Yi H, Zhang B, Huang W. Flotillin-2 promotes cell proliferation via activating the c-Myc/BCAT1 axis by suppressing miR-33b-5p in nasopharyngeal carcinoma. *Aging*. 2021;13(6):8078–8094. doi:10.18632/aging.202726
33. Chen YY, Ho HL, Lin SC, Hsu CY, Ho DM. Loss of BCAT1 expression is a sensitive marker for IDH-mutant diffuse glioma. *Neurosurgery*. 2019;85(3):335–342. doi:10.1093/neuros/nyy338
34. Tonjes M, Barbus S, Park YJ, et al. BCAT1 promotes cell proliferation through amino acid catabolism in gliomas carrying wild-type IDH1. *Nat Med*. 2013;19(7):901–908. doi:10.1038/nm.3217
35. Luo L, Sun W, Zhu W, et al. BCAT1 decreases the sensitivity of cancer cells to cisplatin by regulating mTOR-mediated autophagy via branched-chain amino acid metabolism. *Cell Death Dis*. 2021;12(2):169. doi:10.1038/s41419-021-03456-7
36. Papathanassiu AE, Ko JH, Imprialou M, et al. BCAT1 controls metabolic reprogramming in activated human macrophages and is associated with inflammatory diseases. *Nat Commun*. 2017;8(1):16040. doi:10.1038/ncomms16040
37. Xie Y, Gao L, Xu C, et al. ARHGEF12 regulates erythropoiesis and is involved in erythroid regeneration after chemotherapy in acute lymphoblastic leukemia patients. *Haematologica*. 2020;105(4):925–936. doi:10.3324/haematol.2018.210286
38. Springelkamp H, Iglesias AI, Cuellar-Partida G, et al. ARHGEF12 influences the risk of glaucoma by increasing intraocular pressure. *Hum Mol Genet*. 2015;24(9):2689–2699. doi:10.1093/hmg/ddv027
39. Xing XQ, Li B, Xu SL, Liu J, Zhang CF, Yang J. MicroRNA-214-3p regulates hypoxia-mediated pulmonary artery smooth muscle cell proliferation and migration by targeting ARHGEF12. *Med Sci Monit*. 2019;25:5738–5746. doi:10.12659/MSM.915709
40. Zheng Y, Ouyang Q, Fu R, et al. The cyclohexene derivative MC-3129 exhibits antileukemic activity via RhoA/ROCK1/PTEN/PI3K/Akt pathway-mediated mitochondrial translocation of cofilin. *Cell Death Dis*. 2018;9(6):656. doi:10.1038/s41419-018-0689-4.
41. Li G, Liu L, Shan C, et al. RhoA/ROCK/PTEN signaling is involved in AT-101-mediated apoptosis in human leukemia cells in vitro and in vivo. *Cell Death Dis*. 2014;5(1):e998. doi:10.1038/cddis.2013.519.